Science Journal of Kanagawa University **34** : 1-7 (2023)

■ Full-Length Paper ■ By a grant from Research Institute for Integrated Science, Kanagawa University

Local Atomic Structures around Implanted Phosphorus Atoms in Diamond Analyzed by X-ray Absorption Near Edge Structure

Yasushi Hoshino[1, 2, 4], Yuhei Seki[2] and Kei Mitsuhara[3]

[1] Department of Science, Faculty of Science, Kanagawa University, Yokohama City, Kanagawa 221-8686, Japan
[2] Research Institute for Integrated Science, Kanagawa University, Yokohama City, Kanagawa 221-8686, Japan
[3] Ritsumeikan Global Innovation Research Organization, Ritsumeikan University, Kusatsu City, Shiga 525-8577, Japan
[4] To whom correspondence should be addressed: E-mail: yhoshino@kanagawa-u.ac.jp

Abstract: Formation of highly controlled p-type and n-type conductive layers in diamond by ion implantation technique has been strongly desired for realizing diamond-based electronic devices for decades; however practically available doping condition has not been found especially in n-type doping. In this study, we comprehensively determined the local structures and depth profiles of implanted P atoms as n-type dopant to find out the origin of inactivation of implanted P atoms. The local structure around the implanted P atoms was analyzed by X-ray absorption fine structure using synchrotron-radiation-light and the first-principle calculation based on density functional theory. We found at least four components for all prepared samples in the near edge X-ray absorption structure, suggesting that implanted P atoms locate in four different chemical environments. We eventually assigned all the components by comparing the simulated X-ray absorption with the first-principle theoretical calculation: one of the components corresponds to active phosphorus atom in the substitutional site, and others are the elemental P-P bonds and some defect complexes probably acting as inactive species for n-type dopant. These facts suggest that the knowledge of local structure of implanted P atoms and control of them are substantially important to reduce the inactivation factors of the implanted dopants.
Keywords: ion implantation doping, chemical bonding structure, synchrotron radiation light, X-ray absorption fine structure, DFT calculation

Introduction

Effective impurity doping in diamond especially by ion implantation technique has been one of the crucial issues for realizing electronic power devices. The advantage of ion implantation doping is that the degree of freedom for device design is significantly expanded since one can dope almost all impurity atoms in designated area and depth with an accurate concentration. This fact finally results in short process time, large area doping, and low financial cost in fabricating integrating devices. The ion implantation doping has been therefore successfully used in device fabrications of Si- and GaAs- based semiconductor technology today [1-3]. In the case of diamond semiconductor fabrication, there are so far some reports on ion implantation doping focused on substrate quality, ion implantation conditions, and activation annealing processes; however, electrical activation of doped impurities in diamond by ion implantation has not been sufficiently accomplished yet [4-7]. Quite recently, we succeeded in high-efficient heavy B doping around 10^{19} cm^{-3} concentration by B ion implantation at room temperature (RT) followed by activation annealing at 1150 to 1450 ℃ [8-10]. We consequently realized excellent p-type conductivity and confirmed a typical ionization energy of acceptor B in a wide temperature range from 150 K to 1073 K. The doping efficiency progressed remarkably and reached 78 %, and the Hall mobility at RT was real-

©Research Institute for Integrated Science, Kanagawa University

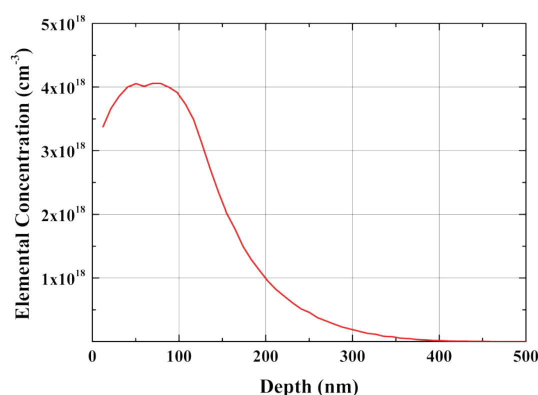

Fig. 1. Observed depth profile of implanted phosphorus atom measured by SIMS.

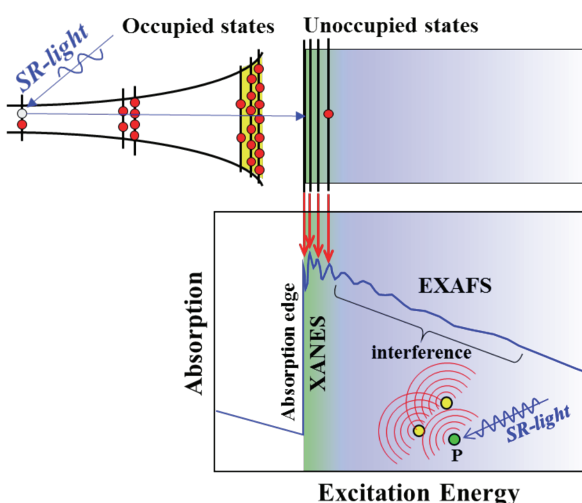

Fig. 2. Schematical concept of X-ray absorption mechanism in an atom and absorption spectrum.

ized to be 108 $cm^2\ V^{-1}s^{-1}$. We also succeeded in fabrication of p-type Schottky barrier diode by all-ion-implantation doping process recently [11, 12].

On the other hand, n-type doping in diamond is the most difficult issues today. It is recognized that phosphorus atom with an ionization energy of about 0.6 eV is now the most probable dopant candidate for n-type impurity in diamond. Gas-phase CVD doping especially on the (111) diamond surface is today the probable way that the practically available properties are somehow realized [13-17]. In the case of ion implantation doping, however, the electrical activation of implanted P atoms has not succeeded yet [18]. Therefore, the investigation of true origin for the electrical inactivation of implanted donor P atoms should be important to realize the effective n-type doping into diamond. Recently, Shikata *et al*. reported local structure of phosphorus atom in (001)- and (111)- oriented diamond by gas-phase doping in CVD analyzed by X-ray absorption spectra; however, they could not narrow down the local structure of doped P atom definitely [19, 20].

In this study, we comprehensively studied the local structures near the implanted impurity P atoms. We carried out P implantation at RT with doping concentrations of 5×10^{18} and 2×10^{19} cm^{-3}, which almost the same condition that we succeeded in the electrical activation of implanted boron. The local structure around the implanted P atoms was analyzed by X-ray absorption near-edge structure (XANES) spectrum using synchrotron-radiation light and the first-principle calculation base on density functional theory (DFT) for electronic structures.

Materials and methods

(001)-oriented type IIa diamond substrates with a typical size of $3\times3\times0.25$ mm^3 purchased from Element Six Ltd were first treated by a typical wet chemical process for diamond surface: dipping in the mixture of sulfuric acid and hydrogen peroxide at 200 ℃ for 30 min followed by diluted ammonia and hydrogen peroxide solution at 80 ℃ for 20 min. The sample was then introduced in a vacuum chamber for P ion implantation. We performed P ion implantation at eight multiple incident energies from 10 to 150 keV to obtain flat doping concentration from near surface to 150 nm with doping concentrations of 5×10^{18} and 2×10^{19} cm^{-3} [21]. The total fluences were 6.2×10^{13} and 2.5×10^{14} cm^{-2}, respectively. The observed depth profile of implanted P atom for the former case evaluated by secondary ion mass spectroscopy (SIMS) method is shown in Figure 1. We then deposited thin SiO_2 film with about 100 nm thick to prevent the degradation of diamond surface and anomalous diffusion of atmospheric species in the following high-temperature activation annealing at 1300 ℃ for 2 h [22]. After the activation annealing, the cap layer was completely eliminated from the surface by dipping diluted HF solution, and the surface was cleaned up again by the typical wet chemical treatment.

Local structure around the implanted P atoms in diamond was analyzed by XANES spectrum using synchrotron-radiation-light. As shown in Fig. 2, XANES spectrum strongly reflects the electronic

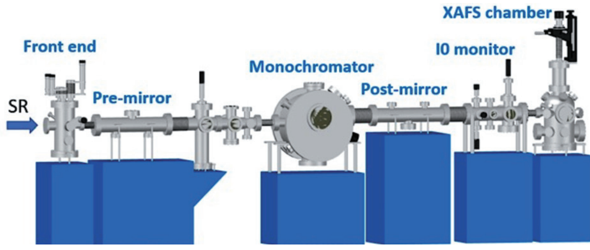

Fig. 3. Schematical view of compact XAFS measurement system in BL-13 at SR-CENTER, Ritsumeikan University.

structure of unoccupied states involving local atomic structure and chemical environment around the excited atom. The XANES spectrum was measured at beam line 13 (BL-13) at SR center, Ritsumeikan University shown in Fig. 3. This beam line mainly consists of three optical systems of front toroidal mirror, Si(111) double crystal monochromator, and post toroidal mirror. One can utilize monochromated SR-light with photon energies from 1200 to 5000 eV, in which the K-shell electron of P with binding energy of ~2100 eV can be effectively excited. The chamber for X-ray absorption measurement is closely set within only 2 m distance from the electron storage ring, allowing us to measure the spectra with excellent statistics: the typical photocurrent on the I_0 monitor mesh was ~100 pA. The energy calibration was carried out by the energy of K absorption edge for the standard $FePO_4$ compound material. The absorption spectra were recorded with two detection modes of total electron yield (TEY) and partial fluorescence yield (PFY) by integrating emitted secondary electrons and characteristic X-ray photons, respectively. The former detection mode is sensitive from surface to ~100 nm depth by integration of photocurrent from the sample. The latter mode provides the information from deeper layers until several μm by a silicon drift detector.

Experimentally obtained XANES spectra were analyzed by comparing with simulated spectra by first-principle calculation by assuming probable local atomic structures. Today, some DFT calculation packages include an option of XANES spectrum calculation. In this study, WIEN2k package was used for self-consistent DFT calculations [23]. The WIEN2k package is known as the most accurate calculation for electronic states especially in core electrons due to all-electron full potential calculation without pseudo-potentials. We employed the generalized gradient approximation by Perdew-Bruke-Ernzerhof (PBE) functional for exchange and correlation potential in Hamiltonian [24, 25]. A Brillouin zone sampling with $4\times4\times4$ grid for wave vectors were used in the present calculations. In structure optimization, we repeatedly carried out the calculation until the Hellmann-Feynman force and energy were well converged. It took typically several days with a high-performance workstation for sequential simulation of each local structure.

Results

Figure 4 shows XANES spectra detected by TEY (a) and PFY (b) mode for the samples with different doping concentrations of 5×10^{18} and 2×10^{19} cm^{-3}. For reference, simulated XANES spectrum of substitutionally doped P is also shown in Fig. 4. Here, we focus on the near-edge absorption structure appearing between 2140 to 2160 eV, which is strongly influenced from the local atomic structure of doped P atom. It is clearly found that four components denoted by A, B, C, and D are observed in all spectra, suggesting that implanted P atoms locate in four

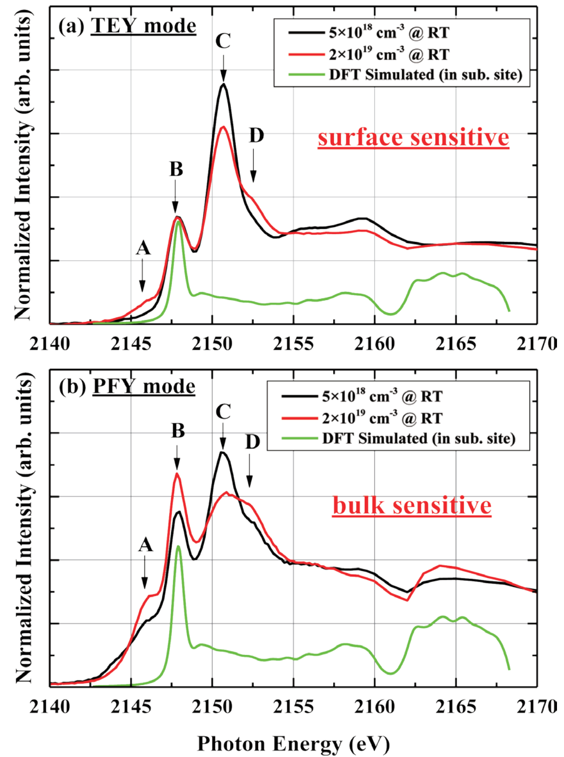

Fig. 4. Experimentally observed XANES spectra of the K-absorption edge observed for the samples in various implantation conditions. The curve drawn with green color denotes simulated spectra by DFT calculation assumed by the local structure of substitutionally doped P atom.

different chemical environments. Compering the peak and dip structures observed in the experimental spectrum to those in the simulated spectrum assumed by substitutional P structure (green curve), the component B is assigned to the substitutional P atom. The relative peak intensity for the component C at the surface sensitive condition (TEY mode) is found to be strongly increased. On the other hand, peak A and D are apparently bulk sensitive. As increasing the doping concentration, the intensities of A and D components are increased and that of C is decreased. The origin of XANES spectra and depth profiles of these components are discussed below.

In order to precisely interpret the XANES spectra,

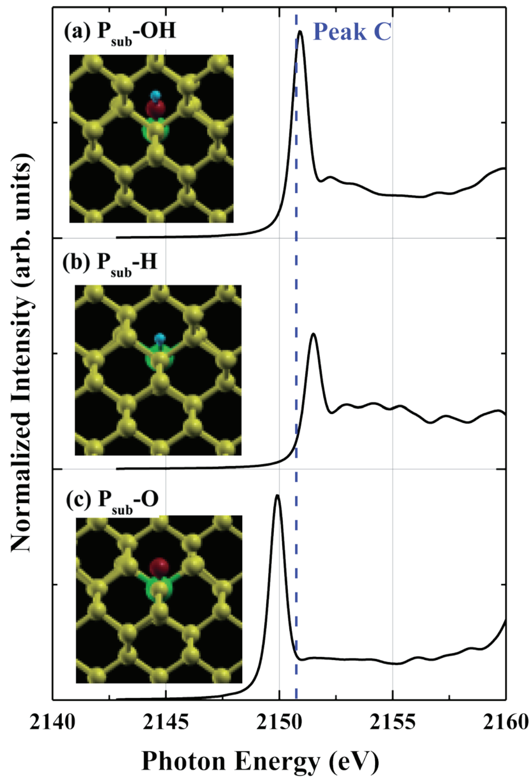

Fig. 5. Simulated XANES spectra assumed by the most probable hydroxyl complexes of (a) P_{sub}-OH, (b) P_{sub}-H, and (c) P_{sub}-O. The blue dashed line denotes the energy position of observed peak C component.

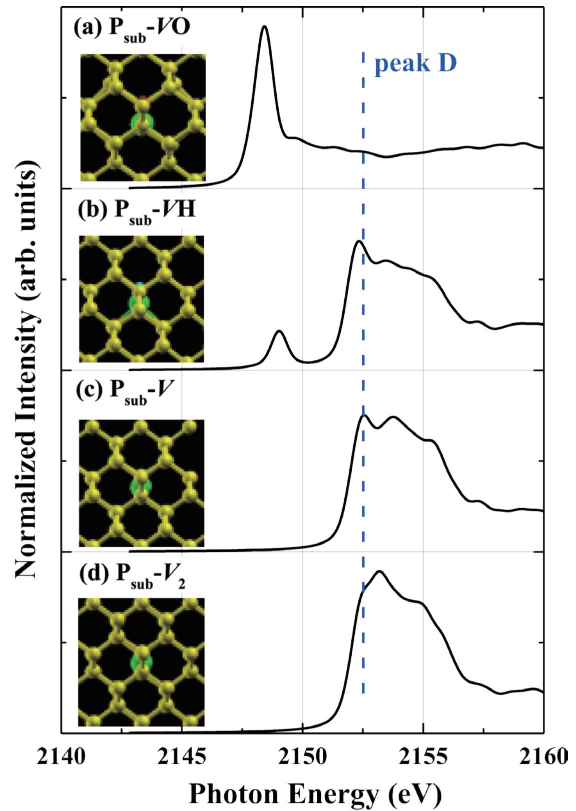

Fig. 6. Simulated XANES spectra for three typical vacancy complex structures of (a) P_{sub}-VO, (b) P_{sub}-VH, (c) P_{sub}-V, and (d) P_{sub}-V_2. The blue dashed line denotes the energy position of observed peak D component.

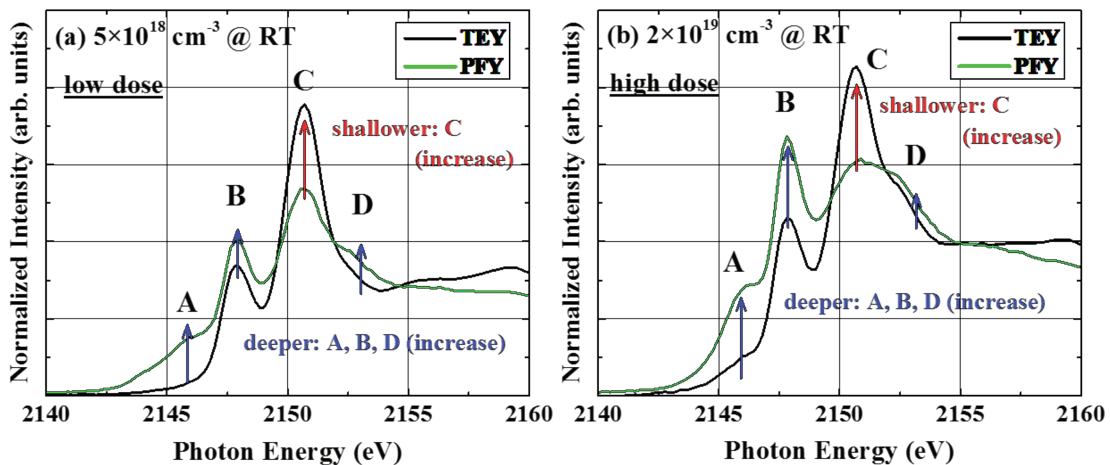

Fig. 7. Depth profile analysis by comparing XANES spectra observed for the sample at RT implantation measured by two detection modes of TEY and PFY.

we performed DFT calculations and compared the experimentally observed spectrum structures to simulated ones. Figure 5 shows simulated XANES spectra assumed by some probable hydroxyl complexes of (a) OH bonded with substitutional P (P_{sub}-OH), (b) H bonded with substitutional P (P_{sub}-H), and (c) O bonded with substitutional P structures (P_{sub}-O). The atomic configuration images after energetically minimized final structures projected along [110] axis are also shown in this figure. It is clearly seen that the energy position of peak C in the experimental XANES spectra (2150.5 eV) is very close to that of the P_{sub}-OH structure or mixture of P_{sub}-H and P_{sub}-O structure, suggesting that the peak C component probably consists of hydroxyl complexes.

Figure 6 shows simulated XANES spectra for four typical vacancy (V) complex structures of (a) VO complex bonding with substitutional P (P_{sub}-VO), (b) VH complex bonded with substitutional P (P_{sub}-VH), (c) V bonding with substitutional P (P_{sub}-V), and (d) divacancy (V_2) bonding with substitutional P (P_{sub}-V_2). The energy positions of the main peak for P_{sub}-VH, P_{sub}-V and P_{sub}-V_2 are found to be significantly close to that of peak D. This small component at the highest energy corresponds to phosphorus and vacancy complexes.

As already mentioned above, we measured XANES spectra by two detection modes of TEY and PFY. TEY mode is surface sensitive and detects the information within about 100 nm in depth and PFY mode detects the information in deeper region until several μm depth, which allows us to analyze the depth profiles of the local structures. Figure 7 shows XANES spectra observed by TEY and PFY modes for the samples with (a) low doping concentration (5×10^{18} cm^{-3}) and (b) high doping concentration (2×10^{19} cm^{-3}) formed by P implantation at RT. It is clearly found that the relative intensity of peak C increased significantly in shallower region for both samples of low and high dosages. On the other hand, the intensities of peak A and B significantly increased in the deeper region. The intensity of peak D was slightly increased in the deeper area and also by higher dosage. On the other hand, K-absorption edge for black and red phosphorus was observed around 2145−2147 eV according to the previous reports, indicating that peak A locating at the lowest energy can be assigned to P-P bonds [26, 27]. Finally, estimated peak energy and probable local structure of each component are summarized in Table 1.

Discussion

According to the XANES spectra and DFT calculation, most of implanted P atoms are existent in the substitutional site, though most of them preferably form defect complexes. Since the peak intensities of B and C were respectively decreased and increased in the shallower area alternatively, it is suggested that substitutionally arranged P atoms near the surface region were preferably bonded with interstitial hydroxyl defects. These hydroxyl species locating near surface region are probably diffused from surface during annealing process via irradiation defects. Furthermore, vacancy-complex structures are distributed around deeper area and significantly increased with increasing ion fluence. It is quite reasonable that ion implantation of heavy elements with higher dosage generally creates many defects and self-clusters in deeper area.

Table 1. Estimated peak energy and probable local structure for observed components in XANES spectra

component	energy (eV)	local structure
A	2145.7	P clusters
B	2147.8	Substitutional site
C	2150.5	OH complex
D	2152.3	Vacancy complex

It is readily predicted that termination of impurity P in substitutional site by such interstitial defects of hydroxyl and vacancy complexes should electrically inactivate the function of donor. It is suggested in the previous reports on P doping by CVD method that incorporations of a large amount of H as well as induced vacancies fatally inactivate donor atoms [28, 29]. These facts suggest that the control of local structure around implanted P atoms is substantially important to reduce the inactivation effect of donor properties of dopant. In addition, we show that the technique of synchrotron-radiation X-ray absorption spectroscopy is one of the powerful tools for determine the local structure of doped atoms.

We in summary investigated the local structures and depth profiles of phosphorus atoms doped by ion implantation in various doping conditions. The P implantations were performed at RT with doping concentrations of 5×10^{18} and 2×10^{19} cm^{-3}. The local

structure around the implanted P atoms was analyzed by XANES using synchrotron-radiation light and the most reliable first-principle DFT calculation with WIEN2k code. In the XANES spectra, four components were clearly observed for all prepared samples, indicating that implanted P atoms locate in four different chemical environments. We eventually assigned all the components by comparing the absorption energies between experimental and simulated XANES spectra. As a result, four components are assigned to be P in substitutional site, P bonded with hydroxyl defects, P bonded with vacancies and P clusters. The depth profiles of these components are quite consistent with the features of ion implantation with heavy atoms. The present study strongly suggests the importance of not only the control of local structures around implanted dopants but also the establishment of methodology for determining local atomic structures of dopants.

Acknowledgments

We sincerely appreciate Mr. Yasunao Saito for their special supports in the maintenance of experimental apparatuses. This research was partly supported by a grant from the Research Institute for Integrated Science, Kanagawa University (RIIS202201).

References

1) Wolf S and Tauber RN (1986) *Silicon Processing for the VLSI Era, Vol. 1*. Lattice Press, Sunset Beach, California.
2) Nebel CE and Ristein J (2003) *Thin-film Diamond I, Semiconductors and Semimetals, Vol. 76*. Elsevier Academic Press.
3) Koizumi S, Umezawa H, Perot J and Suzuki M (2018) *Power Electronics Device Applications of Diamond Semiconductors*. Woodhead Publishing, Duxford.
4) Prins JF (2000) Electrical conduction in diamond after vacancy generation by means of carbon-ion implantation. *Appl. Phys. Lett*. **76**: 2095-2097.
5) Vogel T, Meijer J and Zaitsev A (2004) Highly effective p-type doping of diamond by MeV-ion implantation of boron. *Diamond Relat. Mater*. **13**: 1822-1825.
6) Tsubouchi N and Ogura M (2008) Enhancement of Dopant Activation in B-Implanted Diamond by High-Temperature Annealing. *Jpn. J. Appl. Phys*. **47**: 7047-7051.
7) Ueda K and Kasu M (2008) High-pressure and high-temperature annealing effects of boron-implanted diamond. *Diamond Relat. Mater*. **17**: 502-505.
8) Seki Y, Hoshino Y and Nakata J (2019) Remarkable p-type activation of heavily doped diamond accomplished by boron ion implantation at room temperature and subsequent annealing at relatively low temperatures of 1150 and 1300°C. *Appl. Phys. Lett*. **115**: 072103/1-5.
9) Seki Y, Hoshino Y and Nakata J (2020) Electrical properties and conduction mechanisms of heavily B^+-ion-implanted type IIa diamond: effects of temperatures during the ion implantation and postannealing upon electrical conduction. *Jpn. J. Appl. Phys*. **59**: 021003/1-8.
10) Seki Y, Hoshino Y and Nakata J (2021) Extremely high-efficient activation of acceptor boron introduced by ion implantation at room temperature with various doping concentrations in epitaxially synthesized diamond films by chemical vapor deposition. *J. Appl. Phys*. **129**: 195702/1-10.
11) Shigematsu S, Oishi T, Seki Y, Hoshino Y, Nakata J and Kasu M (2021) Schottky barrier diodes fabricated on high-purity type-IIa CVD diamond substrates using an all-ion-implantation process. *Jpn. J. Appl. Phys*. **60**: 050903/1-4.
12) Seki Y, Saha CH, Shigematsu S, Hoshino Y, Nakata J, Oishi T and Kasu M (2023) The improvement of Schottky barrier diodes fabricated only by B ion implantation doping accomplished by refinement of the electrode structure. *Jpn .J. Appl. Phys. in press*.
13) Koizumi S, Kamo M, Sato Y, H. Ozaki and Inuzuka T (1997) Growth and characterization of phosphorous doped {111} homoepitaxial diamond thin films. *Appl. Phys. Lett*. **71**: 1065-1067.
14) Kato H, Yamasaki S and Okushi H (2005) n-type doping of (001)-oriented single-crystalline diamond by phosphorus. *Appl. Phys. Lett*. **86**: 222111/1-3.
15) Penot J, Tavares C, Gheeraert E, Bustarret E, Katagiri M and Koizumi S (2006) Hall electron mobility in diamond. *Appl. Phys. Lett*. **89**: 122111/1-3.
16) Kato H, Yamasaki S and Okushi H (2007) Carrier compensation in (001) n-type diamond by phosphorus doping. *Diamond. Relat. Mater*. **16**: 796-799.
17) Ohtani R, Yamamoto T, Jansssens SD, Yamasaki S and Koizumi S (2014) Large improvement of phosphorus incorporation efficiency in n-type chemical vapor deposition of diamond. *Appl. Phys. Lett*. **105**: 232106/1-3.
18) Tsubouchi N, Ogura M, Watanabe H, Chayahara A and Okushi H (2009) Diamond Doped by Hot Ion Implantation. *Mater. Sci. Forum* **600-603**: 1353-1356.
19) Shikata S, Yamaguchi K, Fujiwara A, Tamenori Y, Yahiro J, Kunisu M and Yamada T (2017) X-ray absorption fine structure study of heavily P doped (111) and (001) diamond. *Appl. Phys. Lett*. **110**: 072106/1-4.
20) Choudhury S, Colnak R, Schulz C, Lieutenant K, Tranchant N, Arnault J-C, Pinault-Thaury M-A, Jomard R, Knittel P and Petit T (2021) Impact of Nitrogen, Boron and Phosphorus Impurities on the Electronic Structure of Diamond Probed by X-ray Spectroscopies. *J. Carbon Res*. **7**: 28/1-10.
21) Ziegler JF, Biersack JP, and Littmark U (1985) *The Stopping and Range of Ions in Solids*. Pergamon, Oxford.
22) Hoshino Y, Seki Y and Mitsuhara K (2022) Local Structures of Phosphorus atoms implanted in Crystalline diamond. *J. Appl. Phys*. **132**: 165704/1-11.
23) Blaha P, Schwarz K, Tran F, Laskowski R, Madsen

GKH and Marks LD (2020) *J. Chem. Phys.* **152**: 074101/1-30.

24) Perdew JP, Burke K and Ernzerhof M (1996) Generalized Gradient Approximation Made Simple. *Phys. Rev. Lett.* **77**: 3865-3868.

25) Perdew JP, Burke K and Ernzerhof M (1997) ERRATA: Generalized Gradient Approximation Made Simple [Phys. Rev. Lett. 77, 3865 (1996)]. *Phys. Rev. Lett.* **78**: 1396.

26) Nicotra G, Politano A, Mio AM, Deretzis I, Hu J, Mao ZQ, Wei J, La Magna A and Spinella C (2016) Absorption edges of black phosphorus: A comparative analysis. *Phys. Status Solidi B* **253**: 2509-2514.

27) Li M, Li W, Chen N, Liang J, Liu Y, Banis MN, Li J, Xiao Y, Gao X, Hu Y, Xiao Q, Doyle-Davis K, Liu Y, Yiu YM, Li D, Liu S, Li R, Brandys F, Divigalpitiya R, Sham T-K and Sun X (2021) Revealing Dopant Local Structure of Se-Doped Black Phosphorus. *Chem. Mater.* **33**: 2029-2036.

28) Hayashi K, Yamanaka S, Watanabe H, Sekiguchi T, Okushi H and Kajimura K (1997) Investigation of the effect of hydrogen on electrical and optical properties in chemical vapor deposited on homoepitaxial diamond films. *J. Appl. Phys.* **81**: 744-753.

29) Mizuochi N, Watanabe H, Isoya J, Okushi H and Yamasaki S (2004) Hydrogen-related defects in single crystalline CVD homoepitaxial diamond film studied by EPR. *Diamond. Relat. Mater.* **13**: 765-768.